C.P. No. 241
(17,693)
A.R.C. Technical Report

C.P. No. 241
(17,693)
A.R.C. Technical Report

MINISTRY OF SUPPLY

AERONAUTICAL RESEARCH COUNCIL

CURRENT PAPERS

Velocity Calculations by Conformal Mapping for Two-Dimensional Aerofoils

By

D. A. Spence and N. A. Routledge

LONDON: HER MAJESTY'S STATIONERY OFFICE

1956

PRICE 6s. 6d. NET

C.P. No. 241

U.D.C. No. 533.691.11.011.3 : 533.69.042.1

Report No. Aero.2539
February, 1955

ROYAL AIRCRAFT ESTABLISHMENT

Velocity calculations by conformal mapping for two-dimensional aerofoils

by

D. A. Spence, (Aerodynamics Dept.)
and
N.A. Routledge, (Mathematical Services Dept.)

SUMMARY

A method is derived for computing the conformal transformation between the plane of an aerofoil of arbitrary shape (symmetrical or cambered), and the plane of its velocity potential at zero lift (in which the aerofoil contour becomes a slit), in order to permit calculations of the velocity at points off the surface. The integral equation which relates the contours is derived by an application of Cauchy's theorem, and solved to the order of the square of thickness ratio. The solution is found by representing the ordinate distribution by a Fourier series. The rapid tailing-off of the Fourier coefficients for all smooth aerofoil shapes then leads to high accuracy being achieved with a comparatively small amount of effort. As an example, the transformation and surface velocity distribution are calculated by this approximate method for a 50 per cent thick Piercy aerofoil, and are found to have an error of less than 1 per cent. Higher accuracy can, of course, be expected for smaller and more realistic thickness ratios. The solution of the inverse problem, of calculating the section shape for a prescribed velocity distribution, by the present method, is also briefly outlined.

The method is straightforward and has proved easy to use as a computing routine.

LIST OF CONTENTS

LIST OF APPENDICES

LIST OF TABLES

LIST OF ILLUSTRATIONS

LIST OF SYMBOLS

$z = x + iy$	complex co-ordinate in physical plane of aerofoil
$\zeta = \xi + i\eta$	complex co-ordinate in slit plane (= potential function for flow at zero lift)
$f(z) = \zeta$	mapping function
y_t, y_c	thickness and camber distributions measured from no-lift direction
$\bar{y}$	ordinate distribution of camber line measured from chord line
ϵ	thickness/chord ratio
a	length of slit in ζ-plane
$f_1(x)$	function defined in equation (33)
$g_1(x) = \frac{df_1}{dx}$	function defined in equation (35)
$f_2(x)$	function defined in equation (41)
α	angle of incidence
α_o	zero-lift angle of cambered section
Δx	chordwise displacement in aerofoil plane of points which coincide on slit (Section 9)
ρ	leading edge radius
τ	trailing edge angle
$\sigma = 2 - \frac{\tau}{\pi}$	
m, n, p, r	integers (suffix p is used for pivotal points) (r is also used as a polar co-ordinate in Appendix B)
N	number of pivotal points
M	number of non-negligible Fourier coefficients
$\theta = \cos^{-1}(2x-1)$	(also used as polar co-ordinates in Appendix B)
$\phi = \cos^{-1}\left(2\frac{\xi}{a} - 1\right)$	
a_r, b_n	Fourier coefficients of aerofoil shape
$k_r = \sum_{n=1}^{N-1-r} n\, a_n\, a_{n+r}$	

LIST OF SYMBOLS (Contd.)

c_n, d_n, e_n	coefficients derived from a_n, k_n (Section 6)	
α_n, β_r	Fourier coefficients used in equations (58), (59) et seq	
x', y', ξ', θ'	dummy variables of integration	
u, v	variables used in equation (27)	
κ, λ, μ	constants	
K	circulation round aerofoil	
q	velocity on aerofoil surface	
R	radius of large contour	Sections 3, 9.1
δ	radius of small semi-circle	Sections 3, 9.1
A, B	constants in transformation of trailing edge region, equation (66)	
σ	angular co-ordinate in ζ-plane	Appendix B
$u(\sigma) = \sigma - \theta$		Appendix B
$g(\zeta)$ = mapping function		Appendix B

1 Introduction

A simple and accurate method is described for calculating the conformal transformation of an aerofoil into a slit along the real axis, and hence for finding velocity distributions in potential flow. An integral equation which determines the transformation is obtained, and its solution found at pivotal points, equally spaced in $\theta = \cos^{-1}(2x-1)$, by representing the shape of the aerofoil as a Fourier series in θ.

The work was undertaken in order to make possible velocity calculations at points off the aerofoil surface, in the trailing edge region, which are required for the prediction of boundary layer effects on lift by the methods of Ref.1. In Section 8 it is shown how, for this purpose, the present transformation may be fitted to the appropriate analytical form near a trailing edge of finite angle τ.

A solution of the mapping problem may, of course, be found to any desired accuracy by the Theodorsen-Garrick[2] method of successive approximations, and the present method will, by the Uniqueness theorem, lead to the same answer. However, the transformed variable is here expanded explicitly as a power series in the thickness ratio, ε say. The method is not adapted to the process of successive approximations, but it gives at once values which seem to be of sufficient accuracy for most purposes (namely, three or four figures of decimals, for aerofoils which are not too thick). This approach is thought to be new.

Retaining only the first two terms of the power series leads to an expression for the velocity which is equivalent to that obtained by Weber[3], but the present Fourier representation enables the third term, in ε^2, to be retained without difficulty. The numerical work, even when this extra term is used, is substantially lighter than that of Ref.3, since it involves fewer multiplications. Moreover, the integral equation connecting the aerofoil with the slit plane has some intrinsic interest.

The greater part of the paper, Sections 2-8, applies only to symmetric sections. For cambered aerofoils, considered in Section 9, the method has not been elaborated beyond the term in ε. To this order of accuracy, it reproduces the known results for no-lift angle, etc. The integral equation in the transformation of a cambered profile contains terms coming from the two points of the aerofoil at different chordwise positions (one on the upper and one on the lower surface), which correspond to a single point of the slit, and calculations correct to the order of ε^2 are rather complicated.

2 An outline of the method (for symmetric sections)

2.1 The transformation of an aerofoil into a slit

Consider a symmetric closed aerofoil C in the complex z-plane, with its chord line along the real axis from 0 (leading edge) to 1 (trailing edge), and let $\zeta = f(z)$ be the unique conformal transformation which takes the region outside C into the region outside a slit, Γ say, extending from 0 to a along the real axis of the complex ζ-plane, such that $\frac{df}{dz} \to 1$ at infinity*. Suppose the points $z = x \pm iy$ of C transform

---

* It is well known (see Ref.11, p.70) that there is one and only one analytic function, defined outside C, which has the required properties.

to the point $\zeta = \xi + io$ of Γ, so that ξ is real. Then it is shown in Section 3 that

$$\frac{dx}{d\xi} = 1 - \frac{1}{\pi}\int_0^1 \frac{dy(x')}{dx'} \cdot \frac{dx'}{\xi - \xi'},$$

or, what is the same,

$$\xi = x + \frac{1}{\pi}\int_0^a \frac{y'\, d\xi'}{\xi - \xi'} + \text{constant}. \qquad (1)$$

The integrals here are Cauchy principal values, and primes are used for dummy variables (so that $\xi' = \xi(x')$ is the point to which the points $x' \pm iy'$ of the aerofoil transform). Also, in the integrals, y is taken positive (for, for any value of x in $(0,1)$ there correspond two values of y for which $x + iy$ lies on C).

Now (1) is an integral equation for ξ in terms of x. If the thickness ratio ε is introduced, by replacing the ordinate $y(x)$ by $\varepsilon\, y(x)$, (so that $y_{max} = \frac{1}{2}$) then the solution of (1) may, it is not unreasonable to assume, be expanded as a power series in ε (valid for suitably small values of ε):

$$\xi = x + \varepsilon\,[f_1(x) - f_1(o)] + \varepsilon^2\,[f_2(x) - f_2(o)] + \ldots \qquad (2)$$

Expressions for $f_1(x)$ and $f_2(x)$ are obtained in Section 4.

Putting $x = 1$, the length of the slit is given by

$$a = 1 + \varepsilon\,[f_1(1) - f_1(o)] + \varepsilon^2\,[f_2(1) - f_2(o)] + \ldots \qquad (3)$$

Then also

$$\frac{d\xi}{dx} = 1 + \varepsilon\frac{df_1}{dx} + \varepsilon^2\frac{df_2}{dx} + \ldots \qquad (4)$$

2.2 The velocity on the aerofoil

In flow at zero incidence with unit velocity at infinity, the velocity along the aerofoil surface is simply $\left|\frac{df}{dz}\right|$, since ζ is the complex velocity potential of the corresponding parallel flow in the ζ-plane. This velocity may be written

$$q = \frac{d\xi}{dx}\left[1 + \varepsilon^2\left(\frac{dy}{dx}\right)^2\right]^{-\frac{1}{2}}. \qquad (5)$$

In flow at incidence α with circulation K. the velocity at a point

$$\xi = \frac{a}{2}(1+\cos\phi) \tag{6}$$

of the slit is easily shown to be

$$\frac{\sin(\phi-\alpha) - \frac{K}{\pi a}}{\sin\phi}, \tag{7}$$

and if K has the Joukowski value

$$K = -\pi a \sin\alpha$$

of ideal fluid theory, this velocity is

$$\cos\alpha + \tan\frac{\phi}{2}\sin\alpha, \tag{8}$$

which may be written

$$\cos\alpha \pm \left(\frac{a-\xi}{\xi}\right)^{\frac{1}{2}}\sin\alpha. \tag{9}$$

Thus the velocity of ideal flow in the aerofoil plane at incidence α is given on the aerofoil by

$$q = \frac{d\xi}{dx}\left[1+\varepsilon^2\left(\frac{dy}{dx}\right)^2\right]^{\frac{1}{2}}\left[\cos\alpha \pm \left(\frac{a-\xi}{\xi}\right)^{\frac{1}{2}}\sin\alpha\right], \tag{10}$$

the $\pm$ signs corresponding to the upper and lower surfaces.

2.21 Velocity at leading edge

If ρ is the leading edge radius, then near the leading edge ($x = \xi = 0$)

$$\varepsilon^2\left(\frac{dy}{dx}\right)^2 = \frac{\rho}{2x}$$

$$\frac{\xi}{x} = \left(\frac{d\xi}{dx}\right)_{L.E.},$$

and equation (10) becomes

$$q_{L.E.} = \left[\frac{2a}{\rho}\left(\frac{d\xi}{dx}\right)_{L.E.}\right]^{\frac{1}{2}}\sin\alpha \tag{11}$$

2.3 The use of Fourier series

The expressions for $f_1(x)$, and other functions which are obtained in Section 4 are Cauchy principal values of certain integrals, and to evaluate them we make the transformation

$$x = \tfrac{1}{2}(1 + \cos\theta) \qquad (\text{for } 0 \leqslant \theta \leqslant \pi) \tag{12}$$

and assume that y is given by a Fourier sine series in θ. For practical purposes a truncated sine series

$$y = \sum_{n=1}^{N}{}' a_n \sin n\theta \qquad (N \text{ even}) \tag{13}$$

can be fitted with high accuracy (see Appendix A). The a_n are in effect co-ordinates of the aerofoil shape, and are obtained from the values, y_p, of y at the $N-1$ points x_p (where

$$\theta = \theta_p = \frac{p\pi}{N}, \qquad p = 1, 2, \ldots, N-1) \tag{14}$$

by the equations

$$a_n = \frac{2}{N}\sum_{p=1}^{N-1}{}' y_p \sin n\theta_p, \quad \text{for } n = 1, \ldots, N-1 \tag{15}$$

(which is, for fixed N, a matrix multiplication). This is shown in Appendix A to give an exact interpolation at the $N-1$ points x_p, and to fit with high accuracy at intermediate points, when y and one or more of its derivatives with respect to θ are continuous in θ.

The functions f_1, $\frac{df_1}{dx}$, etc., and $\frac{dy}{dx}$ (which is not usually known numerically) are then given by trigonometric expressions at the points x_p; e.g.

$$\left(\frac{dy}{dx}\right)_p = -\frac{2}{\sin\theta_p}\sum_{n=1}^{N-1}{}' n a_n \cos n\theta_p, \tag{16}$$

$$f_1(x_p) = \sum_{n=1}^{N-1}{}' a_n \cos n\theta_p. \tag{17}$$

The advantage of specifying the aerofoil by means of the Fourier coefficients a_n is that these tail off very rapidly, and usually all except, say, the first half dozen may be rounded to zero. A comparatively small amount of computation is then involved in evaluating the various functions in the expressions for velocity. Examples showing this rapid convergence are given in Tables I, II and III. Also, these first few non-zero a_n can be found to high accuracy using quite a small number of points in the formula (15) - for instance, $N = 18$ (thus using the values of θ at 10° intervals).

2.4 The relation of the present work to Miss Weber's

Miss Weber obtains an equation ((2 - 12) of Ref.3) for the velocity on the surface of a symmetrical aerofoil at zero incidence, by considering the distribution of singularities necessary to cancel the velocity component of the undisturbed stream normal to the surface. The analysis leading to the equation is exact, certain approximations being made later to simplify the solution. The velocity, as has been pointed out in Section 2.2 above, is simply $\left|\frac{d\zeta}{dz}\right|$, and equating this to Miss Weber's expression leads, after a little reduction, to the integral equation (1). We derive the result in Section 3 by contour integration without reference to singularity distributions. Miss Weber's later approximations are equivalent to retaining only the term in the first order of thickness ratio (the f_1 term in our equation (2)) in the expressions for ξ and $\frac{d\xi}{dx}$, but retaining the $\left(\frac{dy}{dx}\right)^2$ term, which is of the second order (except that it becomes infinite at the leading edge).

The present method is thus very similar to hers in principle, and results obtained by applying both with equal accuracy will not differ by more than a (thickness)^2 term. However, the numerical work is cut considerably by the explicit use of the a_n's, since only the first few of these differ appreciably from zero. Most of the formulae in Ref.3 are of the form

$$S(x_p) = \sum_{n=1}^{N-1} S_{n,p}\, y_n$$

and these involve more work, and are more open to computational errors through cancellation between reasonably large positive and negative terms, than the equivalent sums, such as

$$\sum_{n=1}^{N-1} a_n \cos n\theta_p$$

used here. (Actually, formula (15) is the only one which is open to the above objections - once the computer has safely found the a_n and rounded them off, his task is easy.)

Table III shows the a_n's for R.A.E.104 aerofoil, which were computed using $N = 18$; all except 6 were then rounded-off to zero, so that the remaining operations for computing at 17 pivotal points were

multiplications of vectors containing 6 or fewer elements into a 17 × 6 matrix, $\left\{ \cos \frac{np\pi}{18} \right\}$. As a check on the accuracy, the shape corresponding exactly to these 6 rounded values (i.e. computed from them) has also been tabulated, and is seen to agree very closely with the original shape.

3 The Integral Equation

Let us consider contours C and Γ, and the mapping $\zeta = f(z)$, as in Section 2.1. Then the inverse mapping of the ζ-plane onto the z-plane defines z as a function of ζ.

Consider

$$\oint \frac{\zeta - z}{\xi - \zeta} d\zeta ,$$

where ξ is a fixed real point on the slit Γ, and the integral is taken round the contour $\Gamma_1 + \Gamma_2 + \Gamma_3 + \Gamma_4$, as in Figure 1: Γ_1 is the real axis from $-R$ to $\xi - \delta$, Γ_2 is a small semi-circle of radius δ round ξ, Γ_3 is the real axis from $\xi + \delta$ to R, and Γ_4 is the upper semi-circle $|\zeta| = R$.

The corresponding contour in the z-plane is also shown in Figure 1 - note that the points corresponding to those points of Γ_1 and Γ_3 which are not also points of Γ, lie on the real axis of z. (18)

Now on Γ_4, for large R, since

$$\frac{d\zeta}{dz} \to 1 \quad \text{at infinity} \quad \text{(see Section 2.1)}$$

$$z = \zeta + \frac{\kappa}{\pi i} + O\left(R^{-1}\right), \quad \text{for some constant } \kappa ,$$

so that

$$\frac{\zeta - z}{\xi - \zeta} = \frac{\kappa}{\pi i \zeta} + O\left(R^{-2}\right) \tag{19}$$

Thus

$$\lim_{R \to \infty} \int_{\Gamma_4} \frac{\zeta - z}{\xi - \zeta} d\zeta = \kappa \tag{20}$$

Also,

$$\lim_{\delta \to 0} \int_{\Gamma_2} \frac{\zeta - z}{\xi - \zeta} d\zeta = -\pi i \times (\text{Residue of } \frac{\zeta - z}{\xi - \zeta} \text{ at } \zeta = \xi)$$

$$= \pi i \left(\xi - z_0\right) \tag{21}$$

where z_o is the point on the upper side of C corresponding to $\zeta = \xi$.

But, since $\frac{\zeta - z}{\xi - \zeta}$ has no singularities inside or on $\Gamma_1 + \Gamma_2 + \Gamma_3 + \Gamma_4$, then by Cauchy's theorem

$$\int_{\Gamma_1+\Gamma_2+\Gamma_3+\Gamma_4} \frac{\zeta - z}{\xi - \zeta}\, d\zeta = 0 . \tag{22}$$

Therefore, from (20), (21) and (22)

$$\pi i\,(z_o - \xi) - \kappa = \lim_{R\to\infty,\,\delta\to 0} \int_{\Gamma_1+\Gamma_3} \frac{\zeta - z}{\xi - \zeta}\, d\zeta . \tag{23}$$

If we take imaginary parts in this equation, then, recalling that $y' = 0$ for $\xi' < 0$, $\xi' > a$, (18), we have

$$\pi(x - \xi) + \lambda = - P \int_0^a \frac{\varepsilon\, y'\, d\xi'}{\xi - \xi'} , \tag{24}$$

where $x + i\varepsilon y$ is the point on the upper half of C corresponding to $\zeta = \xi$, $x' + i\varepsilon y'$ that for $\zeta = \xi'$, and P indicates the Cauchy Principal value of the integral.

$$(\lambda = \text{imaginary part of the constant } -\kappa) . \tag{25}$$

Thus

$$\xi = x + \frac{\varepsilon}{\pi} P \int_0^a \frac{y'\, d\xi'}{\xi - \xi'} + \text{constant} . \tag{26}$$

(This is essentially equation (1).)

Now here is a well known result (see Ref.4, Appendix I, equation (37) with $n = 1$) concerning differentiation of Cauchy Principal values:

$$\frac{d}{du} P \int_{u_1}^{u_2} \frac{f(v)\, dv}{u - v} = P \int_{u_1}^{u_2} \frac{df(v)}{dv} \frac{dv}{u - v} + \frac{f(u_1)}{u - u_1} - \frac{f(u_2)}{u - u_2} . \tag{27}$$

Applying this to (26) we have, since $y' = 0$ for $\xi' = 0$ and for $\xi' = a$

$$1 = \frac{dx}{d\xi} + \frac{\varepsilon}{\pi} P \int_0^a \frac{dy'}{\xi - \xi'} . \tag{28}$$

4 The evaluation of the coefficients of the first two powers of ε

The integrals in this section are all Cauchy Principal Values, and so the symbol P will be dropped. Equation (28) is then

$$1 = \frac{dx}{d\xi} + \frac{\varepsilon}{\pi} \int_{\xi'=0}^{a} \frac{dy'}{\xi - \xi'} \tag{29}$$

where $\xi = a$ corresponds to $x = 1$. (30)

Also equation (25) becomes

$$\xi = x + \frac{\varepsilon}{\pi} \left[\int_0^a \frac{y' \, d\xi'}{\xi - \xi'} + \int_0^a \frac{y'}{\xi'} \, d\xi' \right], \tag{31}$$

since the origins correspond.

We shall solve equation (31) by finding approximate values for ξ (in terms of x), substituting them in the right hand side of (31), and using the result as a closer approximation.

A first approximation (obtained by putting $\varepsilon = 0$ in (31)) is $\xi = x$, which leads to the second approximation

$$\xi = x + \frac{\varepsilon}{\pi} \left[\int_0^1 \frac{y' \, dx'}{x - x'} + \int_0^1 \frac{y'}{x'} \, dx' \right],$$

$$= x + \varepsilon \left[f_1(x) - f_1(0) \right] \tag{32}$$

say, where

$$f_1(x) = \frac{1}{\pi} \int_0^1 \frac{y' \, dx'}{x - x'}. \tag{33}$$

Now, by Mangler's result already quoted (equation (27)),

$$\frac{d}{dx} f_1(x) = \frac{1}{\pi} \int_{x'=0}^{1} \frac{dy'}{x - x'}, \tag{34}$$

The third approximation to ξ is therefore given by

$$\xi = x + \frac{\varepsilon}{\pi}\int_0^1 \frac{y'\,(1+\varepsilon\, g_1')}{x - x' + \varepsilon\,(f_1 - f_1')}\,dx' + \text{const.} \qquad (37)$$

where $f_1' = f_1(x')$ etc.

Thus, expanding $1 + \varepsilon\,\dfrac{f_1 - f_1'}{x - x'}$, $\left(= \dfrac{\xi - \xi'}{x - x'} + O(\varepsilon^2)\right)$ in the numerator, we obtain

$$\xi = x + \frac{\varepsilon}{\pi}\int_0^1 \frac{y'\,dx'}{x - x'} + \frac{\varepsilon^2}{\pi}\int_0^1 \frac{y'\,dx'}{x - x'}\left[g_1' - \frac{f_1 - f_1'}{x - x'}\right]$$

$$+ \text{const.} \qquad (38)$$

(neglecting terms in $\varepsilon^3, \ldots$)

The last term on the right does not have a singularity at $x' = x$, (from (35)). The integrand is thus bounded and may be integrated by parts.

Thus, re-writing (38)

$$\xi = x + \varepsilon\, f_1(x) - \frac{\varepsilon^2}{\pi}\int_0^1 y'\,dx'\,\frac{d}{dx'}\left(\frac{f_1 - f_1'}{x - x'}\right) + \text{const.}, \qquad (39)$$

$$= x + \varepsilon\, f_1(x) + \frac{\varepsilon^2}{\pi}\int_0^1 \frac{f_1 - f_1'}{x - x'}\,\frac{dy'}{dx'}\,dx' + \text{const.}, \qquad (40)$$

by parts, (since $y(o) = y(1) = 0$).

Thus

$$\xi = x + \varepsilon\,[f_1(x) - f_1(o)] + \varepsilon^2\,[f_2(x) - f_2(o)]\,, \qquad (2)$$

say, where

$$f_2(x) = \frac{1}{\pi}\int_0^1 \frac{f_1 - f_1'}{x - x'}\,\frac{dy'}{dx'}\,dx'\,, \qquad (41)$$

since the origins of x and ξ correspond.

5 The evaluation of $f_1(x)$ and $f_2(x)$

With the expressions (12) and (13) for x and y, $f_1(x)$ and $f_2(x)$ may be expressed as functions of θ, using the well-known results for Cauchy Principal values:

If $n > 0$,

$$\frac{1}{\pi}\int_0^{\pi} \frac{\sin n\theta' \sin \theta' \, d\theta'}{\cos \theta' - \cos \theta} = -\cos n\theta , \tag{42}$$

and

$$\frac{1}{\pi}\int_0^{\pi} \frac{\cos n\theta' \, d\theta'}{\cos \theta' - \cos \theta} = \frac{\sin n\theta}{\sin \theta} , \tag{43}$$

(see, for instance, Ref.5, Appendix I).

5.1 An expression for $f_1(x)$

Now $f_1(x)$ is, by definition,

$$\frac{1}{\pi}\int_0^{1} \frac{y' \, dx'}{x - x'} \qquad \text{(see (33))}.$$

Thus, writing

$$\left.\begin{aligned} y' &= \sum_{n=1}^{N-1} a_n \sin n\theta' \\ \text{and} \\ x' &= \tfrac{1}{2}(1 + \cos \theta') \end{aligned}\right\} \quad \text{(after (12) and (13))},$$

(33) becomes

$$f_1(x) = -\frac{1}{\pi}\sum_{n=1}^{N-1} a_n \int_0^{\pi} \frac{\sin r\theta' \sin \theta' \, d\theta'}{\cos \theta' - \cos \theta} \tag{44}$$

or

$$f_1(x) = \sum_{n=1}^{N-1} a_n \cos n\theta , \qquad \text{by (42)} . \tag{45}$$

Clearly then

$$\frac{df_1}{d\theta} = -\sum_{n=1}^{N-1} n\, a_n \sin n\theta , \tag{46}$$

and so

$$\frac{df_1}{dx} = 2 \sum_{n=1}^{N-1} n\, a_n \left(\frac{\sin n\theta}{\sin \theta} \right) . \tag{47}$$

5.2 An expression for $f_2(x)$

The definition of $f_2(x)$ was

$$f_2(x) = \frac{1}{\pi} \int_{x'=0}^{1} \frac{f_1(x) - f_1(x')}{x - x'} \, dy(x') \quad \text{(by (41))}.$$

Now

$$dy(x') = \sum_{n=1}^{N-1} n\, a_n \cos n\theta' \, d\theta' , \tag{48}$$

and, from (45),

$$f_1(x) - f_1(x') = \sum_{m=1}^{N-1} a_m (\cos m\theta - \cos m\theta') . \tag{49}$$

Thus

$$f_2(x) = \sum_{m=1}^{N-1} \sum_{n=1}^{N-1} n\, a_m\, a_n\, I_{m,n} \tag{50}$$

where

$$I_{m,n} = -\frac{2}{\pi} \int_0^{\pi} \cos n\theta' \, \frac{\cos m\theta' - \cos m\theta}{\cos \theta' - \cos \theta} \, d\theta' , \tag{51}$$

$$= \frac{2}{\pi} \cos m\theta \int_0^{\pi} \frac{\cos n\theta'}{\cos \theta' - \cos \theta} \, d\theta'$$

$$- \frac{1}{\pi} \int_0^{\pi} \frac{\cos (m+n)\theta' + \cos (m-n)\theta'}{\cos \theta' - \cos \theta} \, d\theta' , \text{ clearly,}$$

$$= 2 \cos m\theta \, \frac{\sin n\theta}{\sin \theta} - \frac{\sin (m+n)\theta}{\sin \theta} - \frac{\sin |m-n| \, \theta}{\sin \theta} , \tag{52}$$

from (43).

There are two cases to consider:

(1) $\underline{m > n.}$ Then $\sin |m-n| \theta = \sin (m-n) \theta$, so that

$$I_{m,n} = - 2 \frac{\sin (m-n)\theta}{\sin \theta} . \tag{53}$$

(2) $\underline{m < n.}$ Then $\sin |m-n| \theta = - \sin (m-n) \theta$, so that

$$I_{m,n} = 0 . \tag{54}$$

Thus, from (50)

$$f_2(x) = - 2 \sum_{\substack{m=2 \\ m > n}}^{N-1} \sum_{n=1}^{N-2} n a_m a_n \frac{\sin (m-n) \theta}{\sin \theta} \tag{55}$$

If now we write

$$k_r = \sum_{n=1}^{N-1-r} n a_n a_{n+r} , \tag{56}$$

then (55) can be re-written as

$$f_2(x) = - 2 \sum_{r=1}^{N-2} k_r \frac{\sin r\theta}{\sin \theta} . \tag{57}$$

5.3 Evaluating $\frac{df_1}{dx}$, f_2 and $\frac{df_2}{dx}$

We have seen from (57) and (47) that f_2 and $\frac{df_1}{dx}$ are of the form

$$\sum_{n=1}^{M} \alpha_n \frac{\sin n\theta}{\sin \theta} . \tag{58}$$

$$\sum_{n=0}^{M-1} \beta_n \cos n\theta \qquad (59)$$

for certain constants β_n .

Then

$$2 \sum_{n=1}^{M} \alpha_n \sin n\theta = 2 \beta_o \sin \theta + \sum_{n=1}^{M-1} 2 \beta_n \cos n\theta \sin \theta ,$$

$$= 2 \beta_o \sin \theta + \sum_{n=1}^{M-1} \beta_n (\sin (n+1) \theta - \sin (n-1) \theta). \qquad (60)$$

Comparing the coefficients of $\sin n\theta$ on both sides of (60) we have:

$$\left.\begin{aligned} \beta_{M-1} &= 2 \alpha_M \\ \beta_{M-2} &= 2 \alpha_{M-1} \\ \beta_{M-3} - \beta_{M-1} &= 2 \alpha_{M-2} \\ \beta_{M-4} - \beta_{M-2} &= 2 \alpha_{M-3} \\ &\cdots\cdots \\ &\cdots\cdots \\ \beta_2 - \beta_4 &= 2 \alpha_3 \\ \beta_1 - \beta_3 &= 2 \alpha_2 \\ 2 \beta_o - \beta_2 &= 2 \alpha_1 \end{aligned}\right\} \qquad (61)$$

The equations (61) can be solved for $\beta_{M-1}, \beta_{M-2}, \ldots, \beta_1, \beta_o$ successively when the values of $\alpha_M, \ldots, \alpha_1$ are known. (In practice it is simpler to find $\beta_{M-1}, \beta_{M-3}, \beta_{M-5}, \ldots$ and then $\beta_{M-2}, \beta_{M-4}, \ldots$)

To evaluate $\frac{df_1}{dx}$ and f_2 it is best to express them in the form (59) before doing any computation. Then if

$$f_2(x) = \sum_{n=0}^{N-3} d_n \cos n\theta \qquad (62)$$

we have also

$$\frac{df_2}{dx} = 2\sum_{n=1}^{N-3} n\, d_n \frac{\sin n\theta}{\sin \theta} \quad . \tag{63}$$

We can then express (63) in the form (59) by the above process, and obtain

$$\frac{df_2}{dx} = \sum_{n=0}^{N-4} e_n \cos n\theta \,, \quad \text{say.} \tag{64}$$

6 The Numerical Procedure

(1) Choose the number of pivotal points N to be used. (The choice of N depends on the accuracy required. For the first N-1 Fourier sine coefficients to be reliable, the last four must be negligible to the required degree of accuracy.)

(2) Calculate (or read from a graph) the values of $y_p = y(x_p)$, where $x = \frac{1}{2}(1+\cos\theta_p)$, and

$$\theta_p = \frac{p\pi}{N} \,, \quad \text{for } p = 1, 2, \ldots, N-1, \quad \text{(see (4))}.$$

(3) Find

$$a_n = \frac{2}{N}\sum_{n=1}^{N-1} y_p \sin n\theta_p \,, \quad \text{for } n = 1,2,\ldots N-1, \quad \text{(see (15))}.$$

(This is best done by setting out the (N-1)th order square symmetric matrix $\left\{\sin \frac{np\pi}{N}\right\}$ and multiplying the vector $\{y_p\}$ into it.) The last few a_n so obtained should be negligible. Choose an integer M such that $a_{M+1}, a_{M+2}, \ldots$ are all negligible, but not a_M. Then take

$$y = \sum_{n=1}^{M} a_n \sin n\theta \qquad \text{(by (13))},$$

and then

$$c_1 = \sum_{n=1}^{M} a_n \cos n\theta \qquad \text{(by (45))}.$$

(4) Make a table of $n\,a_n$ for $n = 1,\ldots,M$. Then

$$\frac{dy}{dx} = -\frac{2}{\sin\theta}\sum_{n=1}^{M} n\,a_n \cos n\theta\ .$$

(5) Find $c_0, c_1,\ldots, c_{M-1}$ from the equations

$$\begin{aligned} c_{M-1} &= 4\,M\,a_M \\ c_{M-2} &= 4\,(M-1)\,a_{M-1} \\ c_{M-3} - c_{M-1} &= 4\,(M-2)\,a_{M-2} \\ &\cdots\cdots \\ c_1 - c_3 &= 4\,.\,2\,a_2 \\ 2\,c_c - c_2 &= 4\,.\,1\,a_1 \end{aligned}$$

Then, from (61) and (47),

$$\frac{df_1}{dx} = \sum_{n=0}^{M-1} c_n \cos n\theta\ .$$

(6) Find

$$k_r = \sum_{n=1}^{M-r} n\,a_n\,a_{n+r}\ , \quad \text{for } r = 1,2,\ldots,M-1.$$

(If a_n and $n\,a_n$ are tabulated in adjacent columns, the calculation of k_r is very simple. The k's taper off much more rapidly than the a's, since they represent double sums; similarly f_2 and $\frac{df_2}{dx}$ are numerically much smaller than f_1 and $\frac{df_1}{dx}$.)

(7) Now find $d_0,\ldots, d_{M-2}$ from the equations

$$\begin{aligned} d_{M-2} &= -4\,k_{M-1} \\ d_{M-3} &= -4\,k_{M-2} \\ d_{M-4} - d_{M-2} &= -4\,k_{M-3} \\ &\cdots\cdots \\ d_1 - d_3 &= -4\,k_2 \\ 2\,d_o - d_2 &= -4\,k_1 \end{aligned}$$

Then

$$f_2(x) = \sum_{n=0}^{M-2} d_n \cos n\theta \ .$$

(8) Now find $e_0, \ldots, e_{M-3}$ from the equations

$$e_{M-3} = 4\,(M-2)\,d_{M-2}$$

$$e_{M-4} = 4\,(M-3)\,d_{M-3}$$

$$e_{M-5} - e_{M-3} = 4\,(M-4)\,d_{M-4}$$

$$\cdots\cdots\cdots$$

$$e_1 - e_3 = 4 \cdot 2\, d_2$$

$$2\,e_0 - e_2 = 4 \cdot 1\, d_1$$

Then, from (61), (63) and (64)

$$\frac{df_2}{dx} = \sum_{n=0}^{M-3} e_n \cos n\theta \ .$$

(9) Then calculate $\frac{dy}{dx}$, f_1, $\frac{df_1}{dx}$, f_2, $\frac{df_2}{dx}$ at $x = 0$, $x = 1$, and at the pivotal points $x = x_p$, $p = 1, \ldots, N-1$, using the expansions of these functions as sine and cosine series given above.

(10) Then, introducing the thickness ratio ε,

$$\xi = x + \varepsilon\,[f_1(x) - f_1(0)] + \varepsilon^2\,[f_2(x) - f_2(0)] \ , \qquad (2)$$

and

$$\frac{d\xi}{dx} = 1 + \varepsilon \frac{df_1}{dx} + \varepsilon^2 \frac{df_2}{dx} \ , \qquad (4)$$

can be computed at $x = 0, 1$ and at the pivotal points.

Then we have $a = \xi\,(1)$ (by (3)).

(12) Then the velocity of ideal flow on the aerofoil surface, at incidence α, by (10), can be computed from the formula

$$\left|\frac{d\zeta}{dz}\right|\left[\cos\alpha \pm \left(\frac{a-\xi}{\xi}\right)^{\frac{1}{2}} \sin\alpha\right]$$

(the $\pm$ signs refer to upper and lower surfaces).

(13) The leading edge radius (at $x = 0$, $\theta = \pi$) is often known a priori, but it can easily be found since, for small $\pi - \theta$

$$y = \varepsilon \sum_{n=1}^{M} (-1)^n \, n \, a_n \, (\pi-\theta) + O\left((\pi-\theta)^3\right) \qquad \text{(from (13))}$$

and

$$x = \tfrac{1}{4}(\pi-\theta)^2 + O\left((\pi-\theta)^4\right) \qquad \text{(from (12))}$$

$$\rho = \lim_{\theta\to 0} \frac{y^2}{2x} = 2\left(\varepsilon \sum_{n=1}^{M} (-1)^n \, n \, a_n\right)^2 .$$

(For the example given in Tables I and II, this gives $\rho = 0.197$, which compares with the exact known value $\rho = 0.200$.)

(14) The velocity at the leading edge, at incidence α, can now be found (from 11). It is

$$\left[\frac{2a}{\rho}\left(\frac{d\xi}{dx}\right)_{x=0}\right]^{\frac{1}{2}} \sin\alpha .$$

6.1 The Inverse Problem - Calculation of shape for a prescribed Velocity Distribution

It has been shown that, correct to order ε, if

$$y = \varepsilon \sum_{n=1}^{N} a_n \sin n\theta$$

then

$$\xi - x = \varepsilon \sum_{n=1}^{N} a_n \cos n\theta$$

i.e. to this order $\xi - x$ is the harmonic conjugate of y. This makes it possible to deduce the aerofoil shape corresponding to a prescribed velocity distribution, correct to order ε.

Suppose $q(x)$ is prescribed, then to the first order in ε, excluding surface curvature,

$$\xi = \int_0^x q(x)\, dx .$$

Thus if $\int_0^x q(x)\, dx - x$ is expressed as a Fourier cosine series, namely

$$\int_0^x q(x)\, dx - x = \Sigma a_n \cos n\theta$$

where $x = \frac{1}{2}(1 + \cos\theta)$, then the corresponding aerofoil shape is given by

$$y = \Sigma a_n \sin n\theta .$$

To allow for surface curvature near the nose, the calculation of shape will require iteration of the above solution, the next approximation being given by fitting a Fourier cosine series to $\xi - x$,

$$= \int_0^x q(x) \left[1 + \left(\frac{dy}{dx}\right)^2\right]^{\frac{1}{2}} dx - x ,$$

where $\left[1 + \left(\frac{dy}{dx}\right)^2\right]^{\frac{1}{2}}$ is calculated from the first approximation. If necessary the above solution could be iterated again.

7 Worked examples

7.1 Piercy aerofoil 50 per cent thick

As a check on the accuracy of the method, it has been applied with $N = 18$ to calculate the transformation and the velocity distribution at zero and 10° incidence, on a Piercy aerofoil 50 per cent thick, whose transformation is known analytically (see Ref.7, pp.212-218). The aerofoil chosen was obtained by taking $\nu = \frac{\pi}{6}$, and $z = \sqrt{3}/2\ z_1$, in the notation of Ref.7, and has a trailing edge angle of $\frac{\pi}{6}$. The results are plotted, together with the aerofoil shape, in Figure 4, and are given in full in Tables I, II. The aerofoil ordinates were computed to 4 places of decimals, and, retaining the same number of figures in the Fourier co-ordinates a_n, k_n (which rounded to 0 after 14 and 6 terms respectively), four-figure agreement with the exact values was found (Table I). The calculation was then carried out retaining three figures only (Table II). In this case a_n, k_n rounded to 0 after 7 and 2 terms respectively, and the points shown as squares in Figure 4 were obtained. The accuracy is still extraordinarily high for such a thick aerofoil, and the labour relatively light. A few points obtained by the Weber method are also included in the figure.

7.2 R.A.E. 101 and 104 aerofoils

The method has been applied to calculate the transformation and velocity distribution for these two members of the R.A.E. family of symmetrical aerofoils (Ref.8). The calculations were actually performed using $N = 18$, but the Fourier coefficients a_n are of course independent of the number of pivotal points (provided they are not too few). To illustrate this, the coefficients calculated by using $N = 8$, $N = 16$, and $N = 18$ are given for the 101 aerofoil in Table III, and are seen to agree with each other to well within the accuracy of the computing method. The table also lists the remaining coefficients k_n, c_n, d_n and e_n for these two aerofoils. For the 104 aerofoil, the shape recalculated from the rounded-off values of a_n is also given in the table, and the velocity at zero incidence and the relation between ξ and x is plotted in Figure 5 for three thickness ratios $\varepsilon = 0.15$, 0.10, 0.06. (These aerofoils are being used for calculations of boundary layer lift reduction factors, to be issued in Ref.9.)

7.3 Ellipto-Cubic Aerofoil with discontinuity in Slope

For smooth shapes such as the Piercy aerofoil, the sine series, besides being an exact interpolation at the pivotal points, fits with very high accuracy at intermediate positions (see Ref.10, Chapters 7-10). An example was therefore calculated to see how much the shape represented by the sine series would differ from the true shape for an aerofoil with a discontinuity in slope. The profile chosen had its front half circular and rear half cubic, with a discontinuity in slope of $\cot^{-1}(1/3)$ at $x = 0.50$, and a point of inflexion at $x = 0.75$. The Fourier sine coefficients for interpolating to this shape are tabulated, and the computed shape compared with the exact shape, in Figure 6. The maximum discrepancy is about 4 per cent, close to the discontinuity, and is produced by the non-uniform convergence at this point of the Fourier series for $\frac{dy}{dx}$ (Gibbs' phenomenon). The computed pressure distribution would thus be expected to be reasonably accurate over the greater part of the profile, but not near the kink (where in any case viscosity effects would predominate in the real flow).

8 Calculation of velocity off the aerofoil surface

This method of conformal transformation was developed in the course of an attempt to relate the neighbourhood of $\zeta = a$ in the slit plane to the neighbourhood of $z = 1$ in the aerofoil plane, in order to perform calculations of the type described in Ref.1, where the circulation round an aerofoil with boundary layers is obtained from a relation between the velocities at two points off the surface of the aerofoil, namely the points at the outer edges of the upper and lower boundary layers at the trailing edge.

For an aerofoil of trailing edge angle τ, the transformation in the neighbourhood of the trailing edge must be approximately that which takes the tangents at the trailing edge into the slit, namely

$$\frac{\zeta}{a} - 1 = A\,(z-1)^{2/\omega}, \tag{65}$$

say, where

$$\omega = 2 - \frac{\tau}{\pi}, \tag{66}$$

or more accurately,

$$\frac{\zeta}{a} - 1 = A\,(z-1)^{2/\omega}\,[1 + B\,(z-1) + \ldots] \qquad (67)$$

(Fig.2). Thus if the relation between ζ and z is known at several points on the surface near the trailing edge, the constants A, B, ... may be fitted, and the velocity at points off the surface but close to the trailing edge may be found from the corresponding velocity in the slit plane.

For points on the aerofoil surface

$$z - 1 = x - 1 + iy,$$

and

$$\frac{\zeta}{a} - 1 = \frac{\xi}{a} - 1 = \left(1 - \frac{\xi}{a}\right) e^{i\pi} .$$

In particular, for aerofoils with zero curvature near the trailing edge - e.g. the R.A.E. family, which are wedge shaped over their rear quarter or so,

$$z - 1 = (x-1)\left(1 - i \tan\frac{\tau}{2}\right) \qquad (68)$$

$$= (1-x)\sec\frac{\tau}{2}\, e^{i(\pi - \tau/2)}$$

and

$$1 - \frac{\xi}{a} = A\left[(1-x)\sec\frac{\tau}{2}\right]^{2/\omega} . \qquad (69)$$

Hence A is evaluated by identifying ξ and x at one point near the trailing edge between equations (2) and (69), and calculations at points off the surface can proceed by the method of Section 3 of Reference 1. This is discussed more fully in a report to be issued later[9]. It has been found, for 101 and 104 aerofoils of several thicknesses, that, correct to 3 figures, the same value of A is obtained for a given profile by identifying (2) and (69) at $\theta = \frac{p\pi}{18}$, for $p = 1, 2, 3,$ or 4. This is an indication of the consistency of the method. A lies between 0.9 and 1.0 for these aerofoils with ε between 0.15 and 0.06.

9 Cambered aerofoils

This section can only be regarded as an outline of the extension of the present method to a contour of general shape which does not possess a line

now correspond in general <u>two</u> points, z_1 and z_2 say, of C. Exactly as in Section 3, we consider

$$\oint \frac{\zeta - z}{\xi - \zeta} d\zeta ,$$

taken in this case round the contour $\Gamma_1 + \Gamma_2 + \ldots \Gamma_7$ shown in Fig.7.

As before, since there is no circulation

$$z = \zeta + \frac{\kappa}{\pi i} + O(R^{-1})$$

at large distances. (Circulation would introduce a logarithmic term, causing the integral round Γ_7 to diverge.) The limits of the integrals round Γ_2, Γ_5 and Γ_7 are respectively

$$2\kappa, \quad \pi i (\xi - z_1), \quad \pi i (\xi - z_2), \tag{70}$$

and since

$$\oint_{\Gamma_1 + \ldots \Gamma_7} \frac{\zeta - z}{\xi - \zeta} d\zeta = 0, \tag{71}$$

we obtain

$$\pi i (z_1 + z_2 - 2\xi) - 2\kappa = \lim_{R \to \infty,\ \delta \to 0} \int_{\Gamma_1 + \Gamma_3 + \Gamma_4 + \Gamma_6} \frac{\xi' - z'}{\xi - \xi'} d\xi' \tag{72}$$

Writing $z_1 = x_1 + i\varepsilon y_1$, $z_2 = x_2 + i\varepsilon y_2$ on the left, and corresponding expressions on the right, we obtain

$$\pi i (x_1 + x_2 - 2\xi) - \pi\varepsilon (y_1 + y_2) - 2\kappa$$

$$= P \int_0^a \frac{\xi' - x_1' - i\varepsilon y_1'}{\xi - \xi'} d\xi' - P \int_0^a \frac{\xi' - x_2' - i\varepsilon y_2'}{\xi - \xi'} d\xi' , \tag{73}$$

where, as in Section 3, $z = \zeta + \frac{\kappa}{\pi i} + O(R^{-1})$ at infinity. Equating real and imaginary parts yields

$$\varepsilon\,(y_1 + y_2) + \text{const} \;=\; \frac{1}{\pi}\int_0^a \frac{x_1' - x_2'}{\xi - \xi'}\,d\xi' \;, \tag{74}$$

$$(x_1 + x_2 - 2\xi) + \text{const} \;=\; -\,\varepsilon\,\frac{1}{\pi}\int_0^a \frac{y_1' - y_2'}{\xi - \xi'}\,d\xi' \;, \tag{75}$$

respectively.

Now

$$y_1 - y_2 \;=\; 2\,y_t \;, \tag{76}$$

the thickness distribution considered in the earlier part of the paper; we may write also

$$y_1 + y_2 \;=\; 2\,y_c + \text{const} \tag{77}$$

where y_c is the camber distribution measured from the no-lift direction. We may introduce also the term

$$\Delta x \;=\; \tfrac{1}{2}\,(x_1 - x_2) \tag{78}$$

for the relative displacement of points on the aerofoil surface which correspond to the same point on the slit. In the symmetrical case, clearly $\Delta x = 0$, so that equation (74) is identically zero, and (75) reduces to the equation already studied, namely

$$2\,(x-\xi) + \text{const} \;=\; -\,\varepsilon\,\frac{2}{\pi}\int_0^a \frac{y_t'}{\xi - \xi'}\,d\xi' \tag{79}$$

which is the same as (1).

In the unsymmetrical case, to obtain a solution correct to order ε we are entitled to replace $y_1(x_1)$, $y_2(x_2)$ by $y_1(x)$, $y_2(x)$ respectively on the left hand side of (74), where,

$$x, \;=\; \tfrac{1}{2}\,(x_1 + x_2), \tag{80}$$

is also the first approximation to ξ, according to (75).

Use may now be made of the result (27) for differentiating Cauchy integrals, (since Δx necessarily vanishes at $\xi = 0$, a, the two ends of the slit). We obtain

$$\varepsilon\,\frac{dy_c}{d\xi} \;=\; \frac{1}{\pi}\int_0^a \frac{d\,(\Delta x')}{\xi - \xi'} \;. \tag{81}$$

(81) is an integration for Δx, which will be solved in Section 9.3.

9.2 Fourier representation of cambered shape

In the general case, with $x = \frac{1}{2}(1+\cos\theta)$, the "upper" surface of the aerofoil corresponds to θ in $(0,\pi)$ and the "lower" to θ in $(\pi, 2\pi)$. We may then replace the whole contour by a series of the form (A.6):

$$y(\theta) = \sum_{n=1}^{\infty} a_n \sin n\theta + \tfrac{1}{2} b_o + \sum_{n=1}^{\infty} b_n \cos n\theta \qquad (82)$$

for θ in $(0,2\pi)$. (The infinite series is written here for the convenience of avoiding the $\frac{1}{2} b_N$ term. In practice b_n's tail off like the a_n's of the earlier sections, and b_N would not enter the computation.)

Now for θ in $(0,\pi)$

$$y_t = \tfrac{1}{2}(y_1 - y_2)$$

$$= \tfrac{1}{2}[y(\theta) - y(2\pi-\theta)]$$

$$= \sum_{n=1}^{\infty} a_n \sin n\theta \,, \qquad \text{as before.} \qquad (83)$$

Similarly

$$y_c = \sum_{n=1}^{\infty} b_n \cos n\theta \qquad (84)$$

+ a constant, which may without loss of generality be put equal to 0.

9.3 The evaluation of Δx

To evaluate Δx correct to order ε, we replace the integral equation (81) by

$$\varepsilon \frac{dy_c}{dx} = \frac{1}{\pi} \int_0^1 \frac{d(\Delta x')}{x - x'} \,. \qquad (85)$$

Substituting from (84) for y_c, and introducing θ, θ', this becomes

$$\varepsilon \sum_{n=1}^{\infty} n b_n \frac{\sin n\theta}{\sin\theta} = \frac{1}{\pi} \int_0^{\pi} \frac{d(\Delta x')}{\cos\theta' - \cos\theta} \,. \qquad (86)$$

Now comparing (86) with (43), we see that

$$d(\Delta x) = \varepsilon \sum_{n=1}^{\infty} n b_n \cos n\theta , \tag{87}$$

and therefore

$$\Delta x = \varepsilon \sum_{n=1}^{\infty} b_n \sin n\theta . \tag{88}$$

(+ constant, which = 0, since Δx is to vanish at $\theta = 0, \pi$.)

9.4 The velocity on the aerofoil

Correct to order ε, equation (75) may be written as

$$\xi = x - \Delta x + \varepsilon f_1(x) \qquad \text{(upper surface)} \tag{89}$$

$$= x + \Delta x + \varepsilon f_1(x) \qquad \text{(lower surface)} . \tag{90}$$

These give the point on the slit corresponding to points x on upper and lower surfaces respectively. Equally, the velocities on the upper and lower surfaces are respectively

$$\left|\frac{d\zeta}{dz}\right| = \left[1 - \frac{d}{dx}(\Delta x) - \varepsilon \frac{df_1}{dx}\right]\left[1 + \varepsilon^2 \left(\frac{dy}{dx}\right)^2\right]^{-\frac{1}{2}} \tag{91}$$

$$\left|\frac{d\zeta}{dz}\right| = \left[1 + \frac{d}{dx}(\Delta x) + \varepsilon \frac{df_1}{dx}\right]\left[1 + \varepsilon^2 \left(\frac{dy}{dx}\right)^2\right]^{-\frac{1}{2}} \tag{92}$$

These expressions may be evaluated numerically at pivotal points, using the series (45) for $f_1(x)$ and (38) for Δx.

9.5 The no-lift angle

In the foregoing paragraphs the no-lift position has been assumed known. If this is not the case, however, an expression for the no-lift angle measured from any chosen chord line may be deduced from the consideration that $\left|\frac{d\zeta}{dz}\right|$ should be single valued at $\xi = \pi$, to order ε, this requires

$$\frac{d}{d\theta}(\Delta x) = 0 \qquad \text{at} \quad \theta = \pi , \tag{93}$$

Now b_n are the Fourier coefficients of the camber distribution when it is measured from the no-lift direction, and are given by

$$b_n = \frac{2}{\pi}\int_0^{\pi} y_c \cos n\theta \, d\theta. \tag{95}$$

If now y_c is measured from a line at a (small) inclination α_o to this, it has the value

$$\bar{y}_c \text{ (say)}, = y_c - x \tan \alpha, \tag{96}$$

and the cosine coefficients become

$$\bar{b}_n = \frac{2}{\pi}\int_0^{\pi} \bar{y}_c \cos n\theta \, d\theta. \tag{97}$$

Then

$$\left.\begin{aligned} &\bar{b}_n = b_n \quad \text{for} \quad n = 2, 3, \ldots \\ \text{and} \quad &\bar{b}_1 = b_1 - \alpha_o \end{aligned}\right\} \tag{98}$$

(94) may then be written

$$\alpha_o = -\sum_{n=1}^{\infty} n \bar{b}_n, \tag{99}$$

which expresses the direction of the no-lift line relative to a direction fixed in the aerofoil, in terms of the camber distribution measured from this fixed direction.

The standard expression

$$\alpha_o = \frac{1}{\pi}\int_0^{1} \frac{\bar{y}\, dx}{x^{\frac{1}{2}}(1-x)^{3/2}} \tag{100}$$

which is obtained by the first approximation in Ref.2, may easily be shown to be equivalent to (99).

REFERENCES

No.	Author	Title, etc.
1	Spence, D.A.	Prediction of the characteristics of two-dimensional airfoils. Journal Aeronautical Sciences, Vol.21, No.9, Sept. 1954, p.577.
2	Theodorsen, T. and Garrick, I.E.	General potential theory of arbitrary wing sections. NACA Report 452, (1933).
3	Weber, J.	The calculation of the pressure distribution over the surface of two-dimensional and swept wings with symmetrical aerofoil sections. R & M. 2918, July 1953.
4	Mangler, K.W.	Improper integrals in theoretical aerodynamics. ARC Current Paper No.94, 1952. C.P. 94, June 1951.
5	Routledge, N.A.	Evaluating the supersonic drag integral using Fourier Series. RAE Technical Note No. M.S.17, November 1954. ARC 17,503.
6	U.S. Dept. of Commerce	"Tables of Chebychef polynomials $S_n(x)$ and $C_n(x)$." National Bureau of Standards, Applied Maths. Series, No.9, December 1952.
7	Piercy, N.A.V.	"Aerodynamics", 2nd edition. English Universities Press, 1947.
8	Pankhurst, R.C. and Squire, H.B.	Calculated pressure distributions for the RAE 100-104 aerofoil sections. ARC 13254, C.P.80 March 1950.
9	Spence, D.A. and Beasley, J.A.	Calculated lift curve slopes allowing for boundary layer, for the RAE 101 and 104 aerofoils. (To be issued later.)
10	Carslaw, H.S.	"Fourier's Series and Integrals." Macmillan (1921).
11	Carathéodory, C.	"Conformal Representation." Cambridge University Press, 2nd edition (1952).

The following monographs, which are not specifically referred to in the text, provide useful accounts of recent work in the field:

U.S. Dept. of Commerce	"Construction and applications of conformal maps." National Bureau of Standards, Applied Maths. Series, No.18 (1952).
Birkhoff, G., Young, D.M. and Zarantello, E.H.	"Numerical methods in conformal mapping." Proceedings of Symposium Applied Mathematics, Vol.IV "Fluid Dynamics". McGraw-Hill (1953).

APPENDIX A

Interpolation by Fourier Series

Given an integer N, denote $\frac{p\pi}{N}$ by θ_p, for any integer p. Then if $f(\theta)$ is any function, and if for any integer m ($\gtrless 0$)

$$\alpha_m = \frac{1}{2N} \sum_{r=0}^{2N-1} f(\theta_r)\, e^{-im\theta_r}, \tag{A.1}$$

then the function

$$g(\theta) = \sum_{n=-(N-1)}^{N-1} \alpha_n\, e^{in\theta} + \tfrac{1}{2}\left(\alpha_N\, e^{iN\theta} + \alpha_{-N}\, e^{-iN\theta}\right) \tag{A.2}$$

may easily be shown to satisfy

$$f(\theta) = g(\theta) \quad \text{for} \quad \theta = \theta_p, \quad p = 0, 1, 2, \ldots (2N-1). \tag{A.3}$$

If now we put

$$\begin{matrix} a_m \\ b_m \end{matrix} = \frac{1}{N} \sum_{r=0}^{2N-1} f(\theta_r) \begin{matrix} \sin \\ \cos \end{matrix} m\,\theta_r \tag{A.4}$$

then, clearly, $a_o = 0$, $a_N = 0$, and

$$2\,\alpha_{\pm m} = b_m \mp i\, a_m . \tag{A.5}$$

Thus

$$g(\theta) = \tfrac{1}{2} b_o + \tfrac{1}{2} \sum_{n=1}^{N-1} \left[(b_n - i\, a_n)\, e^{in\theta} + (b_n + i\, a_n)\, e^{-in\theta} \right] + \tfrac{1}{4} b_N \left(e^{iN\theta} + e^{-iN\theta}\right)$$

$$= \tfrac{1}{2} b_o + \sum_{n=1}^{N-1} (b_n \cos n\theta + a_n \sin n\theta) + \tfrac{1}{2} b_N \cos N\theta , \tag{A.6}$$

which is the usual way of expressing the interpolating trigonometric polynomial. This full representation is required for the cambered profiles considered in Section 9.

Now, given any function $F(\theta)$, we can define a new function $f(\theta)$ in $(0,2\pi)$ by the rules

$$\left.\begin{aligned} f(o) &= f(\pi) = 0 \\ f(\theta) &= F(\theta) \\ f(2\pi-\theta) &= -F(\theta) \end{aligned}\right\} \quad \text{if} \quad 0 < \theta < \pi \qquad (A.7)$$

(and outside $(0,2\pi)$, $f(\theta)$ can be defined as having period 2π.) For the function $f(\theta)$ it is clear that

$$b_m = 0 \quad \text{for all} \quad m,$$

and that

$$a_m = \frac{2}{N} \sum_{r=1}^{N-1} F(\theta_r) \sin m\theta_r \ . \qquad (A.8)$$

Hence from (A.3) and (A.6) it follows that

$$F(\theta) = \sum_{n=1}^{N-1} a_n \sin n\theta \ , \quad \text{for} \quad \theta = \theta_p, \quad p = 1,2,..(N-1) \ , \qquad (A.9)$$

where the value of a_n is given by (A.8).

The formula (A.9) is the well-known sine interpolation, required in Section 2.3, equations (13), (14) and (15).

A.1 The goodness of the fit in between the pivotal points

(For a good general discussion of this point see Ref.10, Chapters 7-10.)

If $f(\theta)$ is a function of period 2π, and possesses a pth derivative (see footnote), then it is well known (see, for example, Ref.5, Appendix II) that using the formula (A.2) for interpolation at $2N$ points in $(0,2\pi)$ means that for all θ

$$|f(\theta) - g(\theta)| \leq \frac{2}{\pi(p-1)} (N-\tfrac{1}{2})^{-(p-1)} \int_0^{2\pi} |f^{(p)}(\theta)| \, d\theta \ . \qquad (A.10)$$

Footnote: In fact, it is not necessary for f to have p derivatives, but only $(p-1)$; but then, in addition, there must be a function $\phi(\theta)$ such that

When we have a sine series interpolation (using (A.9)), for the periodic function $f(\theta)$ to be continuous (let alone to possess derivatives) it is clearly necessary for $F(\theta)$ to be continuous, and to satisfy

$$F(o) = F(\pi) = 0 .$$

APPENDIX B

A treatment of the mapping problem of nearly circular areas, applying the "direct" approach to the method of Theodorsen and Garrick

Let C be a contour in the complex z-plane, and let $r = e^{F(\theta)}$ be its polar equation

(see Fig. 3(i)). (B.1)

Let Γ be the unit circle in the ζ-plane,

and σ the angular co-ordinate (so that Γ is the curve $\zeta = e^{i\sigma}$)

(see Fig. 3(ii)). (B.2)

Now, let $f(\zeta)$ be any function regular outside and on Γ (and, in particular, regular at infinity, then, if ζ_0 is any point on Γ, we have, from Cauchy's Theorem (using methods similar to those of Section 3),

$$P \oint_{\Gamma} \frac{f(\zeta)\, d\zeta}{\zeta - \zeta_0} + \pi i\, f(\zeta_0) = \oint \frac{f(\zeta)\, d\zeta}{\zeta - \zeta_0}, \tag{B.3}$$

where the latter integral is taken over any large circle, $|z| = R$ say. But the limit of this integral, as $R \to \infty$, is clearly $2\pi i f_\infty$, where f_∞ is the limit of $f(\zeta)$ as $\zeta \to \infty$.

So

$$P \oint_{\Gamma} \frac{f(\zeta)\, d\zeta}{\zeta - \zeta_0} + \pi i\, f(\zeta_0) = 2\pi i\, f_\infty . \tag{B.4}$$

Now, on Γ, $\zeta = e^{i\sigma}$, and $\zeta_0 = e^{i\sigma_0}$, say, so that

$$P \oint_{\Gamma} \frac{f(\zeta)\, d\zeta}{\zeta - \zeta_0} = P \int_0^{2\pi} \frac{f(e^{i\sigma})\, i\, e^{i\sigma}\, d\sigma}{e^{i\sigma} - e^{i\sigma_0}}$$

$$= P \int_0^{2\pi} \frac{f(e^{i\sigma})\, i\, e^{i(\sigma-\sigma_0)/2}\, d\sigma}{2i \sin \frac{1}{2}(\sigma - \sigma_0)}$$

$$= \frac{1}{2} P \int_0^{2\pi} f(e^{i\sigma}) \left(\cot \tfrac{1}{2}(\sigma - \sigma_0) + i\right) d\sigma . \tag{B.5}$$

If we substitute this in (4) and take real parts we have

$$\tfrac{1}{2} P \int_0^{2\pi} \Re f(e^{i\sigma}) \cdot \cot \tfrac{1}{2}(\sigma-\sigma_0)\, d\sigma - \tfrac{1}{2} \int_0^{2\pi} f(e^{i\sigma}) - \pi f(e^{i\sigma_0})$$

$$= -2\pi f_\infty \,. \qquad (B.6)$$

Now let $g(\zeta)$ be an analytic function, such that $g(\zeta)/\zeta$ is regular at infinity, mapping the exterior of Γ on to that of C.

Let us put

$$f(\zeta) = \log (g(\zeta)/\zeta) \,.$$

This is a many-valued function, but we can clearly take one branch of it which is analytic on and outside Γ, and is regular at infinity.

If $\zeta = e^{i\sigma}$, then

$$f(e^{i\sigma}) = \log (e^{F(\theta)+i\theta}/e^{i\sigma})$$

(where $e^{F(\theta)+i\theta}$ is the point on C corresponding to the point $e^{i\sigma}$ on Γ),

$$= F(\theta) + i(\theta-\sigma)$$

(or, at least, we can choose our branch of $f(\zeta)$ so that this is so),

$$= F(\theta) - i\, u(\sigma)$$

(where $u(\sigma) = \sigma - \theta$). (B.7)

Thus, substituting this in (6),

$$\tfrac{1}{2} P \int_0^{2\pi} F(\theta) \cot \tfrac{1}{2}(\sigma-\sigma_0)\, d\sigma + \tfrac{1}{2} \int_0^{2\pi} u(\sigma)\, d\sigma + \pi\, u(\sigma) = -2\pi f_\infty \,. \qquad (B.8)$$

Now, we know (see Ref.11) that there certainly is such a function $g(\zeta)$ (mapping the exterior of Γ on to that of C) and that all such mappings must be of the form $z = g(e^{i\mu}\zeta)$ for some real number μ. It is very easy to see that for one of these transformations $g(e^{i\mu}\zeta)$, (namely that

$$u(\sigma) = -\frac{1}{2\pi} P \int_0^{2\pi} F(\theta) \cot \tfrac{1}{2}(\sigma-\sigma_0)\, d\sigma. \qquad (B.9)$$

(This is the main integral equation of Theodorsen and Garrick (Ref.2).) Thus, to summarise, we know that there is an analytic function $g(\zeta)$, such that $g(\zeta)/\zeta$ is regular at infinity, mapping the exterior of Γ on to that of C, and such that (B.9) holds.

Now, it is well known, and can easily be proved by the Calculus of Residues, that if

$$F(\theta) = F(\sigma - u(\sigma)) \qquad \text{(by (B.7))}$$

$$= \tfrac{1}{2} a_0 + \sum_{n=1}^{\infty} (a_n \cos n\sigma + b_n \sin n\sigma)$$

then

$$-\frac{1}{2\pi} P \int_0^{2\pi} F(\theta) \cot \tfrac{1}{2}(\sigma-\sigma_0)\, d\sigma$$

$$= \sum_{1}^{\infty} (-b_n \cos n\sigma + a_n \sin n\sigma)$$

$$= \mathcal{C} F(\theta),$$

where $\mathcal{C} F(\theta)$ denotes the Fourier Series in σ, conjugate to that for $F(\theta)$.

Thus, from (B.9) and (B.7),

$$\underline{u(\sigma) = \mathcal{C} F(\sigma - u(\sigma))}. \qquad (B.10)$$

Now, if C is nearly circular, $F(\theta)$ will be small and we can derive more and more accurate approximations to $u(\sigma)$ thus (using the approach of Section 4):

(i) $u(\sigma) = 0$.

(ii) $u(\sigma) = \mathcal{C} F(\sigma) = u_1(\sigma)$, say.

(iii) $u(\sigma) = \mathcal{C} F(\sigma - u_1(\sigma))$,

$$\doteq \mathcal{C} F(\sigma) - \mathcal{C}\left[u_1(\sigma) \frac{dF(\sigma)}{d\sigma}\right],$$

$$= u_1(\sigma) + u_2(\sigma) \quad \text{say.}$$

$$\text{(iv)}\quad u(\sigma) = \epsilon F(\sigma - u_1(\sigma) - u_2(\sigma)),$$

$$\doteq \epsilon\left[F(\sigma) - (u_1+u_2)\frac{dF}{d\sigma} + \tfrac{1}{2}(u_1+u_2)^2\frac{d^2F}{d\sigma^2}\right],$$

$$\doteq u_1 + u_2 + \tfrac{1}{2}\epsilon\left[u_1^2\frac{d^2F}{d\sigma^2} - u_2\frac{dF}{d\sigma}\right],$$

$$= u_1 + u_2 + u_3, \text{ say.}$$

Thus, to calculate $u(\sigma)$ (either from (iii) as $u_1 + u_2$, or from (iv) as $u_1 + u_2 + u_3$) we merely need to fit a Fourier Series to $F(\sigma)$ (using the interpolation formulae (A.4) and (A.6)). Then (after rounding some of the coefficients to zero, if this is possible) the Fourier Coefficients of u_1, u_2 and u_3 can be found, from the definitions of u_1, u_2 and u_3, by a few simple additions and multiplications. Thus we obtain the expansion of $u(\sigma)$ as a finite Fourier Series. (It is then possible, as Theodorsen and Garrick have pointed out, in Ref.2, to calculate $\log(g(\zeta)/\zeta)$ at any point outside Γ, very simply, by deriving its power series expansion (in negative powers of ζ) from the Fourier Series for $u(\sigma)$.)

TABLE I

Piercy Aerofoil, ($\varepsilon = 0.5$): 5 Figure Calculation (N = 18)

r	x	εy	εa_n	εf_1	$\varepsilon \frac{dy}{dx}$	$\varepsilon^2 k_n$	$\varepsilon^2 f_2$	ξ	ξ_{exact}	$\frac{d\xi}{dx}$	$\frac{d\xi}{dx}_{exact}$	$\left[1+\left(\frac{dy}{dx}\right)^2\right]^{\frac{1}{2}}$	$\alpha = 0$		$\frac{1.4303-\xi}{\xi}$	$\alpha = 10^3$	
													$q = \left\|\frac{d\xi}{dz}\right\|$	q_{exact}		q	q_{exact}
0	1.00000	0		0.27144	$-\infty$		-0.01696	1.4303	1.4304	1.7857	1.7885	∞	0	0	0	0.8776	0.8783
1	0.99241	0.0547	0.21798	0.26553	-3.5511	0.01219	-0.01702	1.4167	1.4168	1.7851	1.7877	3.6699	0.4864	0.4838	0.0096	1.3409	1.3336
2	0.96985	0.1068	0.06401	0.24835	-1.6737	-0.00232	-0.01725	1.3767	1.3766	1.7803	1.7792	1.9497	0.9131	0.9128	0.0389	1.7033	1.7007
3	0.93302	0.1538	-0.01269	0.21998	-1.004	0.00044	-0.01712	1.3111	1.3113	1.7719	1.7661	1.4145	1.2527	1.2497	0.0909	1.9552	1.9509
4	0.88302	0.1933	0.00300	0.18252	-0.6251	-0.00016	-0.01832	1.2230	1.2235	1.7509	1.7477	1.1793	1.4847	1.4819	0.1685	2.0884	2.0851
5	0.82140	0.2234	-0.00132	0.13770	-0.3715	0.00008	-0.01916	1.1157	1.1165	1.7261	1.7221	1.0668	1.6180	1.6145	0.2820	2.1225	2.1187
6	0.75000	0.2425	0.00079	0.08798	-0.1756	-0.00006	-0.01994	0.9938	0.9946	1.6898	1.6880	1.0153	1.6640	1.6622	0.4392	2.0747	2.0729
7	0.67101	0.2499	-0.00055	0.03642	-0.0182	0.00004	-0.02096	0.8623	0.8631	1.6458	1.6439	1.0002	1.6455	1.6436	0.6587	1.9726	1.9709
8	0.58683	0.2454	0.00035	-0.01468	0.1206	-0.00002	-0.02222	0.7257	0.7268	1.5912	1.5877	1.0072	1.5798	1.5765	0.9709	1.8343	1.8307
9	0.50000	0.2297	-0.00024	-0.06154	0.2374	0.00002	-0.02360	0.5907	0.5918	1.5191	1.5165	1.0278	1.4780	1.4772	1.4214	1.6709	1.6703
10	0.41318	0.2046	0.00017	-0.10172	0.3392	-0.00001	-0.02515	0.4621	0.4636	1.4390	1.4363	1.0560	1.3627	1.3602	2.0952	1.5055	1.5030
11	0.32899	0.1724	-0.00012	-0.13291	0.4225	0.00001	-0.02686	0.3450	0.3465	1.3394	1.3403	1.0856	1.2338	1.2350	3.1458	1.3358	1.3375
12	0.25000	0.1365	0.00010	-0.15381	0.4846	-0.00001	-0.02861	0.2434	0.2450	1.2319	1.2365	1.1113	1.1085	1.1124	4.8763	1.1789	1.1833
13	0.17861	0.1002	-0.00008	-0.16450	0.5290	0.00001	-0.03047	0.1594	0.1604	1.1161	1.1189	1.1313	0.9866	0.9889	7.9730	1.0323	1.0349
14	0.11698	0.0667	0.00005	-0.16607	0.5575	-0.00000	-0.03248	0.0942	0.0951	0.9950	1.0002	1.6437	0.8700	0.8740	14.1837	0.8969	0.9004
15	0.06699	0.0365	-0.00002	-0.16051	0.5682	0.00000	-0.03466	0.0476	0.0481	0.8632	0.8738	1.1502	0.7505	0.7590	29.0483	0.7633	0.7720
16	0.03016	0.0174	0.00003	-0.15080	0.5808	-0.00000	-0.03703	0.0182	0.0183	0.7268	0.7343	1.1564	0.6285	0.6362	77.5879	0.6313	0.6391
17	0.00760	0.0044	-0.00002	-0.14001	0.5458		-0.03982	0.0036	0.0035	0.5319	0.5542	1.1298	0.4708	0.4800	396.3055	0.4677	0.4768
18	0.00000	0		-0.13444	∞		-0.04136	0	0		0	∞	0	0	∞		0

TABLE II

Piercy Aerofoil ($\varepsilon = 0.5$): 3 Figure Calculation

n	x	ε y	ε a_n	ε f_1	$\varepsilon \frac{dy}{dx}$	ε^2 k_n	ε^2 f_2	ξ	ξ_{exact}	$\frac{d\xi}{dx}$	$\frac{d\xi}{dx}$ exact	$\left[1+\right.$
0	1.000	0		0.271	∞		-0.016	1.422	1.430	1.750	1.788	
1	0.992	0.055	0.218	0.265	-3.547	0.012	-0.016	1.412	1.417	1.760	1.788	3.
2	0.970	0.107	0.064	0.248	-1.667	-0.002	-0.016	1.367	1.377	1.780	1.779	1.
3	0.933	0.154	-0.013	0.220	-1.004		-0.017	1.304	1.311	1.785	1.766	1.
4	0.883	0.193	0.003	0.182	-0.622		-0.018	1.213	1.224	1.762	1.748	1.
5	0.821	0.223	-0.001	0.137	-0.366		-0.019	1.107	1.117	1.721	1.722	1.
6	0.750	0.243	0.001	0.089	-0.176		-0.020	0.985	0.995	1.680	1.688	1.
7	0.671	0.250	-0.001	0.037	-0.021		-0.021	0.854	0.863	1.645	1.644	1.
8	0.587	0.245		-0.014	0.118		-0.023	0.718	0.727	1.603	1.588	1.
9	0.500	0.230		-0.062	0.242		-0.024	0.581	0 592	1.534	1.518	1.
10	0.413	0.205		-0.103	0.343		-0.025	0.451	0.461	1.435	1.436	1.
11	0.329	0.172		-0.133	0.419		-0.027	0.335	0.347	1.323	1.340	1.
12	0.250	0.137		-0.154	0.487		-0.028	0.235	0.245	1.216	1.236	1.
13	0.179	0.100		-0.164	0.527		-0.029	0.153	0.160	1.112	1.119	1.
14	0.117	0.067		-0.166	0.523		-0.030	0.087	0.095	0.985	1.000	1.
15	0.067	0.039		-0.161	0.500		-0.031	0.041	0.048	0.815	0.874	1.
16	0.030	0.017		-0.150	0.533		-0.032	0.012	0.018	0.619	0.734	1.
17	0.008	0.004		-0.140	0.506		-0.032	0.000	0.004	0.455	0.554	1.
18	0.000	0		-0.135	∞		-0.032	0	0	0.390	0	

NOTE: The second order terms are simply:

$$\varepsilon^2 f_2 = -0.024 + 0.008 \cos\theta$$

$$\varepsilon^2 \frac{df_2}{dx} = 0.016$$

TABLE III

Fourier and related coefficients for RAE 101 and 104 aerofoils

(1) RAE 104

n	x	y	Recalculated y (from rounded a_n values)	a_n	a_n (Rounded off) (M = 8)	c_n	k_n	d_n	e_n
0	1.0000	0	0			0.644		0.084	0.336
1	0.9924	0.0091	0.010	0.4404	0.440	-1.120	-0.034	0.064	0.416
2	0.9699	0.0359	0.035	-0.1020	-0.102	-0.472	-0.018	0.032	-0.096
3	0.9331	0.0797	0.079	-0.0461	-0.046	-0.304	-0.007	-0.008	0.160
4	0.8830	0.1394	0.139	-0.0128	-0.013	0.080	0.002	0.004	0
5	0.8214	0.2124	0.212	0.0040	0.004	-0.096	0	0	0.096
6	0.7500	0.2971	0.298	0.0005	0	0	0	0.004	
7	0.6710	0.3836	0.384	-0.0009	0	-0.096	-0.001		
8	0.5868	0.4547	0.452	-0.0030	-0.003				
9	0.5000	0.4903	0.490	-0.0007					
10	0.4132	0.4995	0.499	0.0009					
11	0.3290	0.4879	0.490	-0.0009					
12	0.2500	0.4570	0.457	0.0008					
13	0.1786	0.4087	0.408	-0.0019					
14	0.1170	0.3465	0.344	0.0017					
15	0.0670	0.2703	0.278	-0.0014					
16	0.0302	0.2000	0.194	0.0010					
17	0.0076	0.0944	0.103	-0.0009					
18	0	0	0						

(2) RAE 101

n	a_n (N = 8)	a_n (N = 16)	a_n (N = 18)	a_n (Rounded-off) (M = 6)	c_n	k_n	d_n	e_n
0					0.654		0.104	0.088
1	0.4085	0.4084	0.4082	0.408	-1.152	-0.054	0.044	0
2	-0.1469	-0..468	-0.1466	-0.147	-0.324	-0.011	-0.008	0
3	-0.0218	-0.0218	-0.0219	-0.022	0.024	0.003	0	0.064
4	0.0060	0.0056	0.0056	0.006	-0.060	0	0.004	
5	-0.0027	-0.0027	-0.0027	-0.003	-0.072	-0.001		
6	-0.0032	-0.0031	-0.0031	-0.003				
7	0.0010	0.0001	0.0001					
8		-0.0006	-0.0006					
9		-0.0009	-0.0009					
10		0.0002	0.0001					
11		0	-0.0001					
12		-0.0004	-0.0004					
13		0	0					
14		0.0001	0					
15		-0.0002	-0.0002					
16			0					
17			0					
18								

Wt.2078. CP241.K3 - Printed in Great Britain

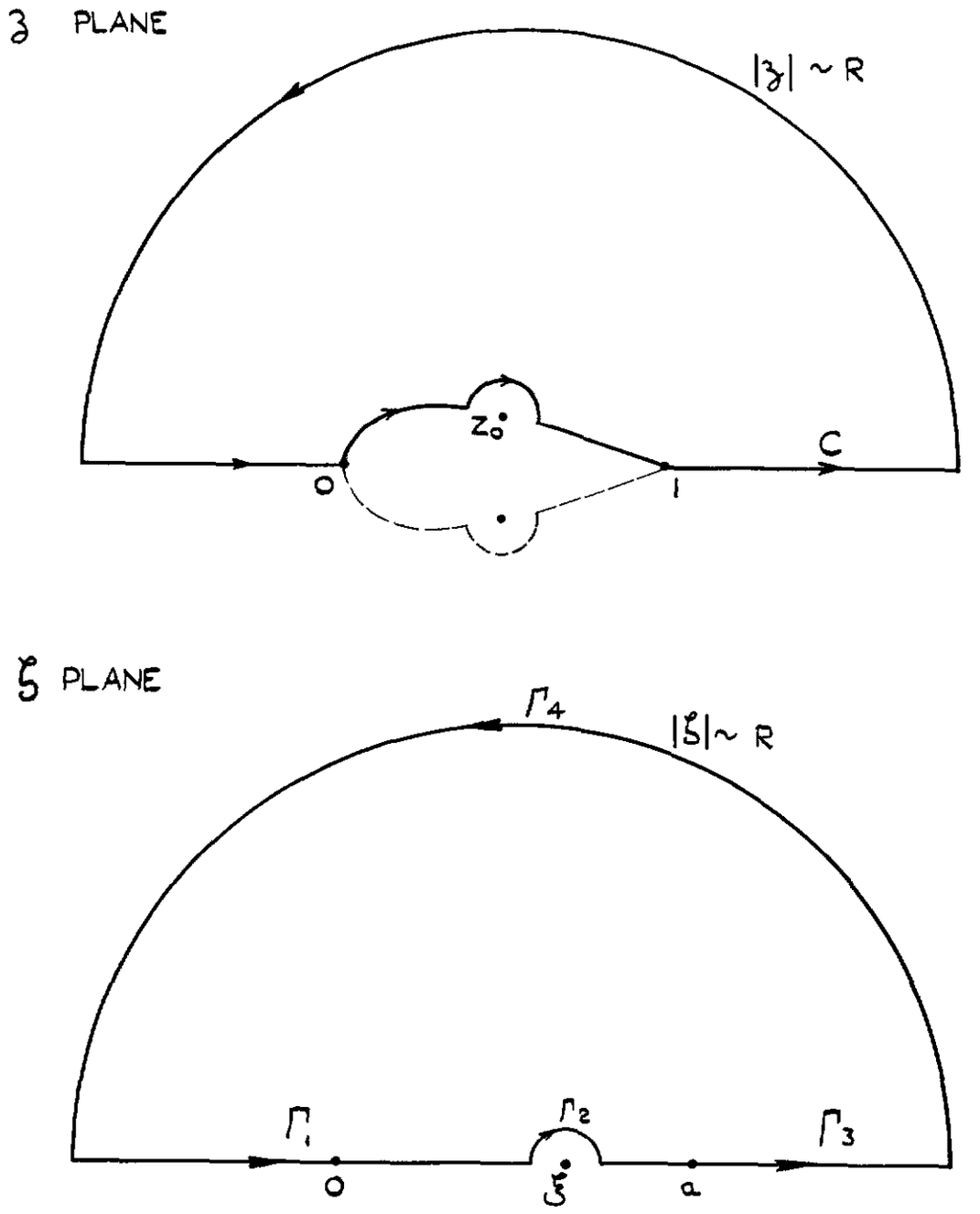

FIG. 1. CONFORMAL TRANSFORMATION OF SYMMETRICAL AEROFOIL TO SLIT.

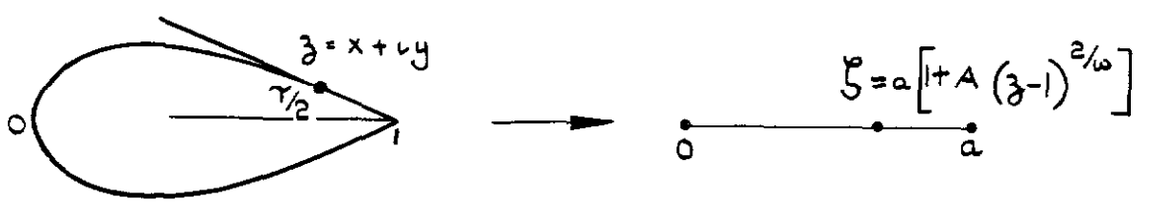

FIG. 2. TRANSFORMATION OF TRAILING EDGE REGION.

FIG. 3.

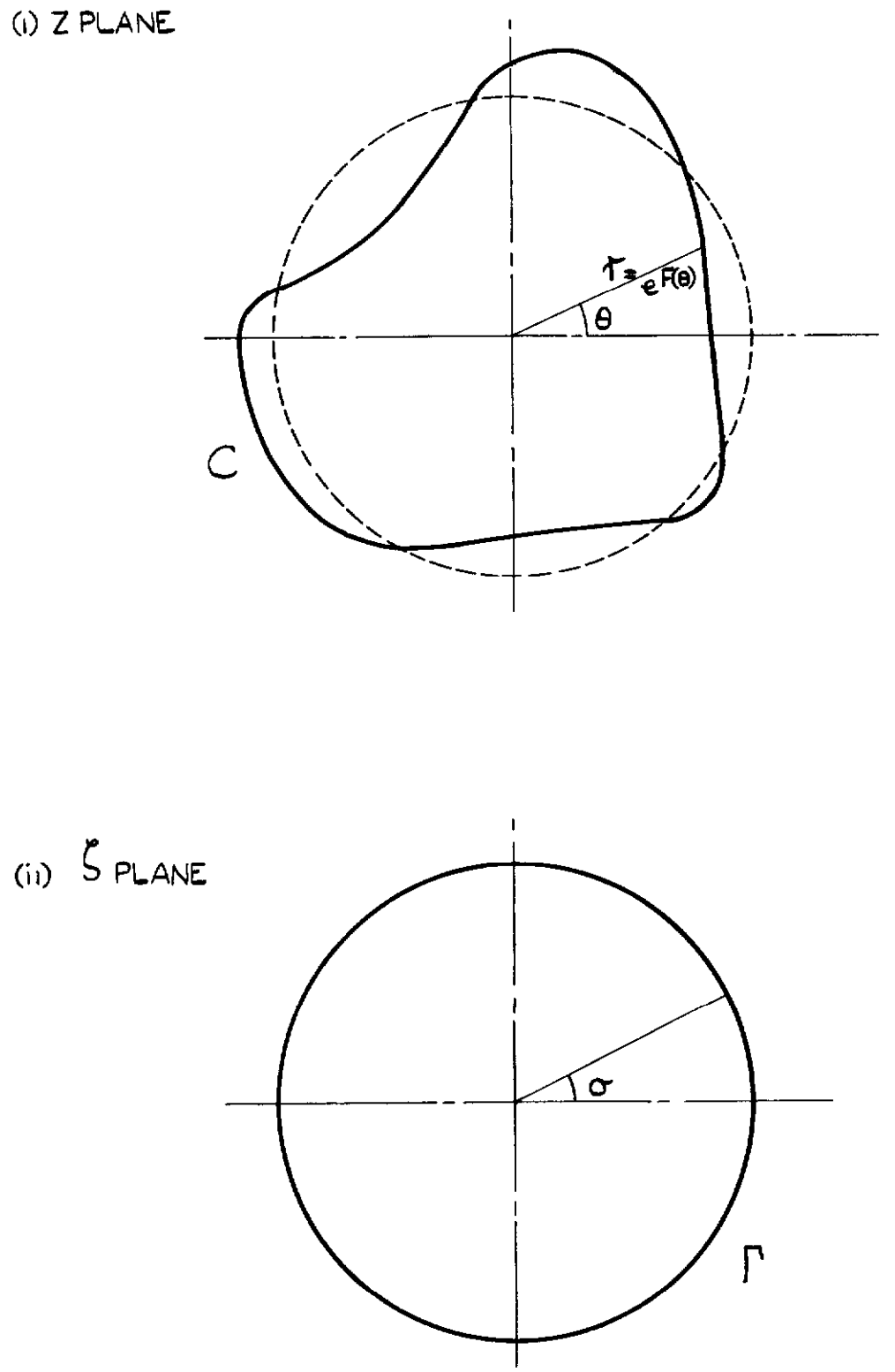

FIG. 3. MAPPING OF NEARLY CIRCULAR AREAS

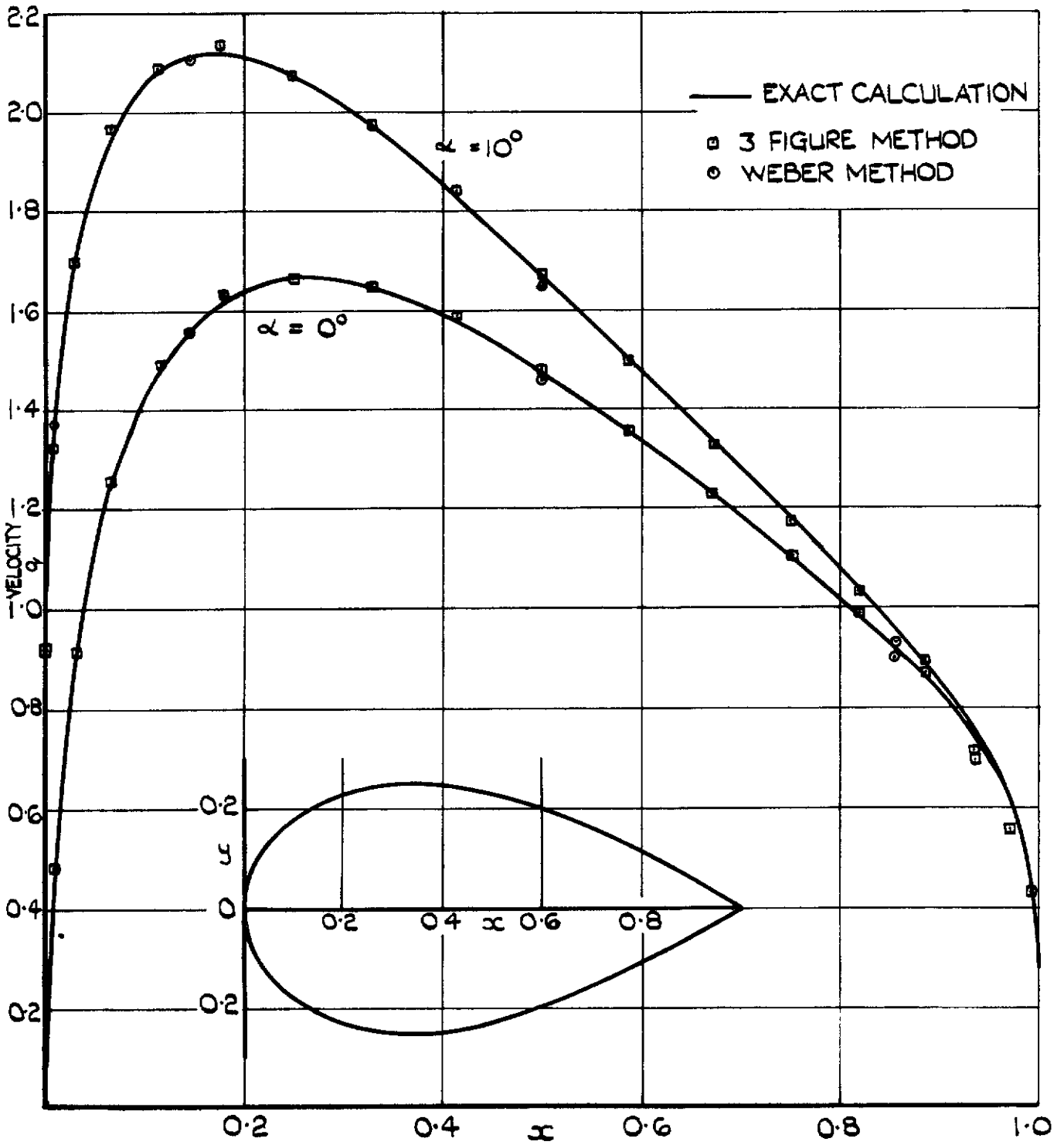

FIG. 4. CALCULATIONS FOR PIERCY AEROFOIL 50 PER CENT THICK.

FIG. 5.(i) &(ii)

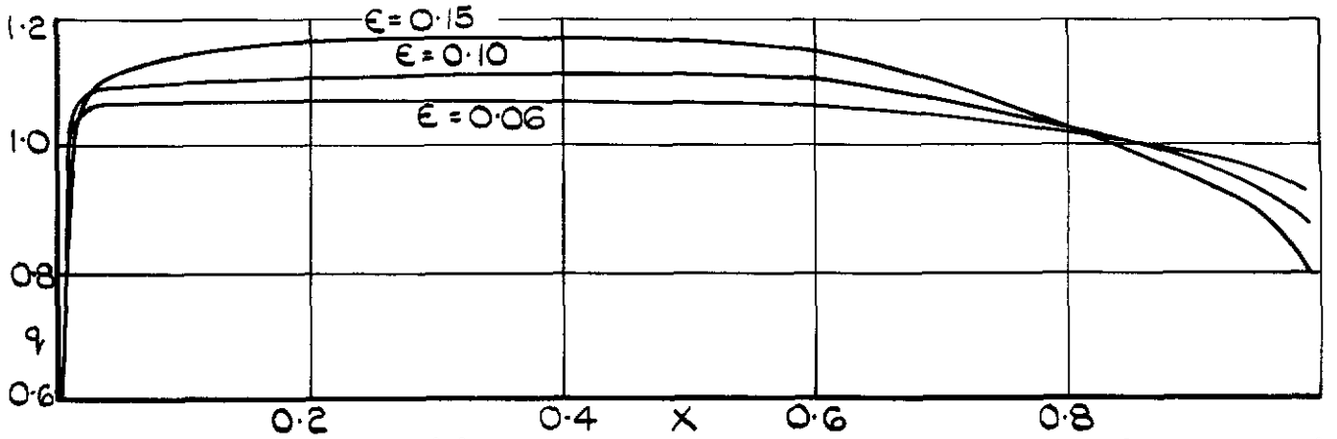

FIG. 5.(ii) VELOCITY DISTRIBUTION AT ZERO INCIDENCE

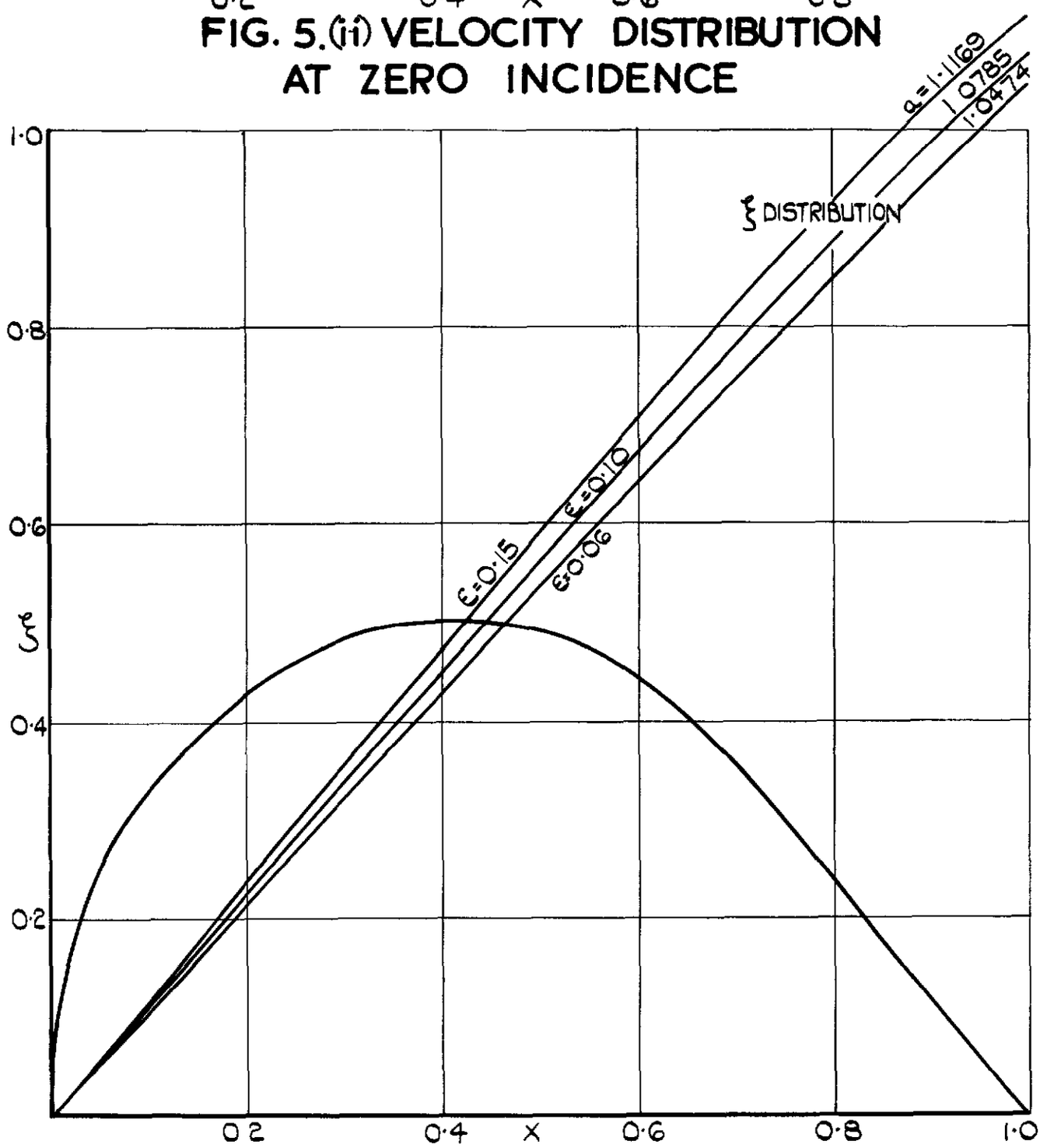

FIG. 5.(i) TRANSFORMATION FOR R.A.E 104 AEROFOIL.

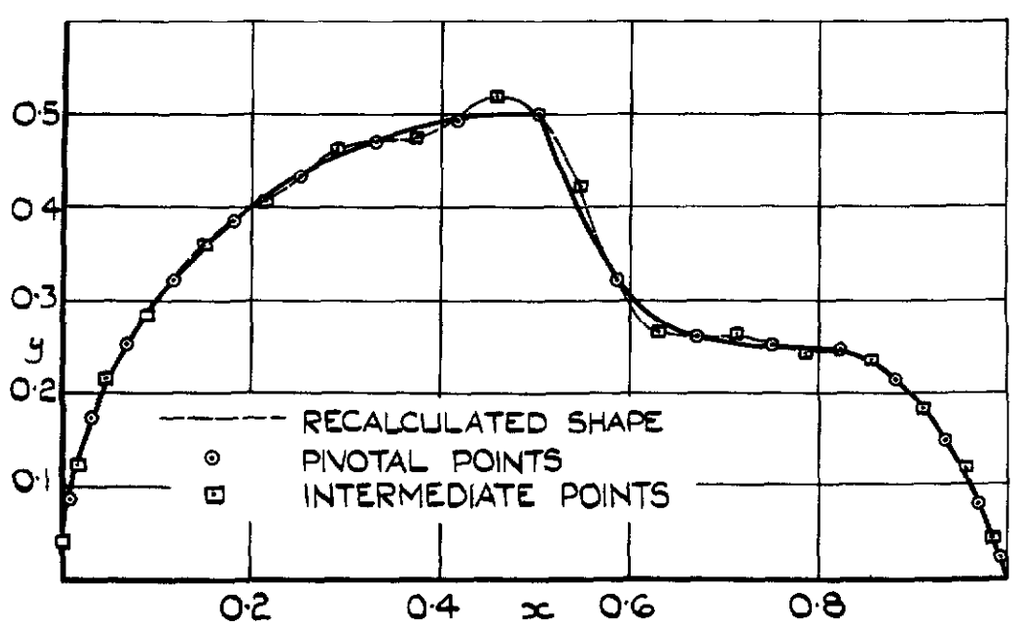

n	a_n
1	0·823
2	-0·170
3	-0·026
4	0·061
5	0·014
6	-0·056
7	-0·046
8	0 012
9	0·024
10	-0·010
11	-0·022
12	0·003
13	0·016
14	-0·003
15	-0·016
16	0·001
17	0·014

FIG. 6. EXACT AND INTERPOLATED ORDINATE DISTRIBUTIONS FOR PROFILE WITH DISCONTINUITY IN SLOPE.

FIG. 7.

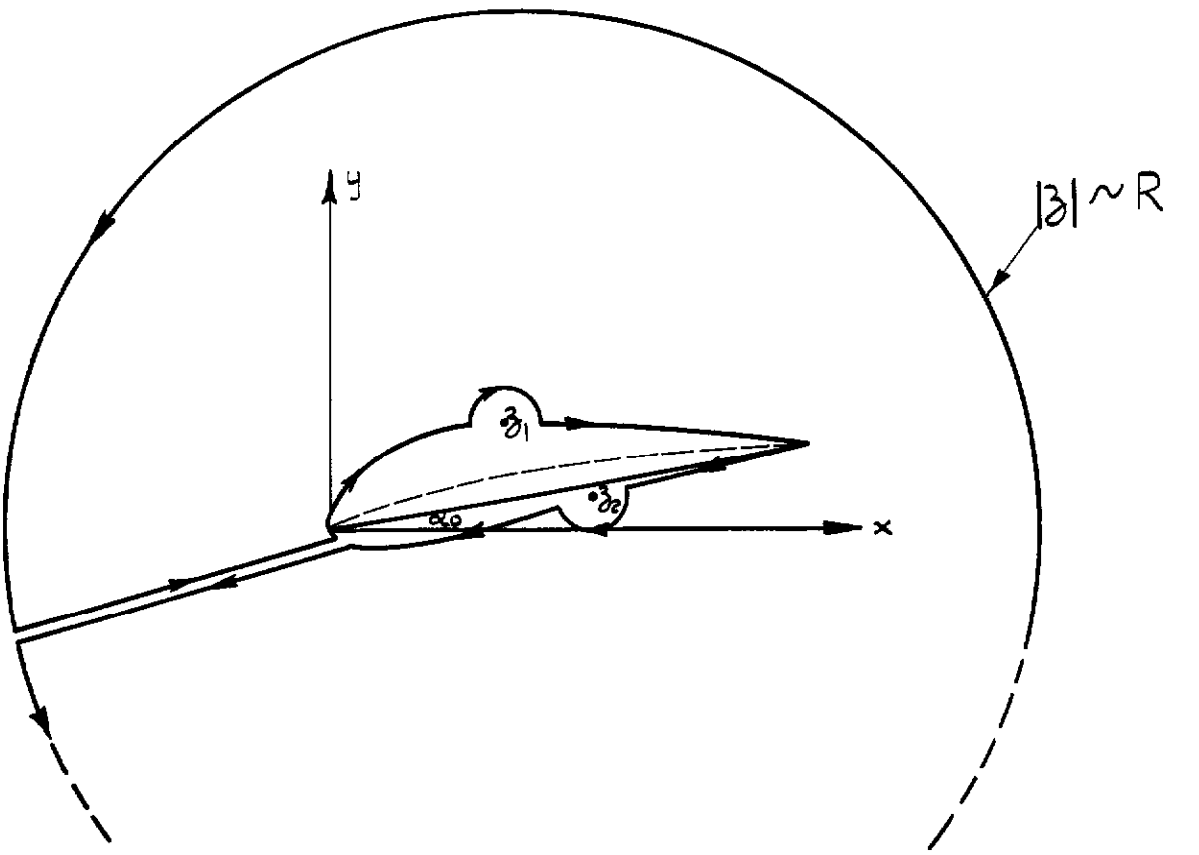

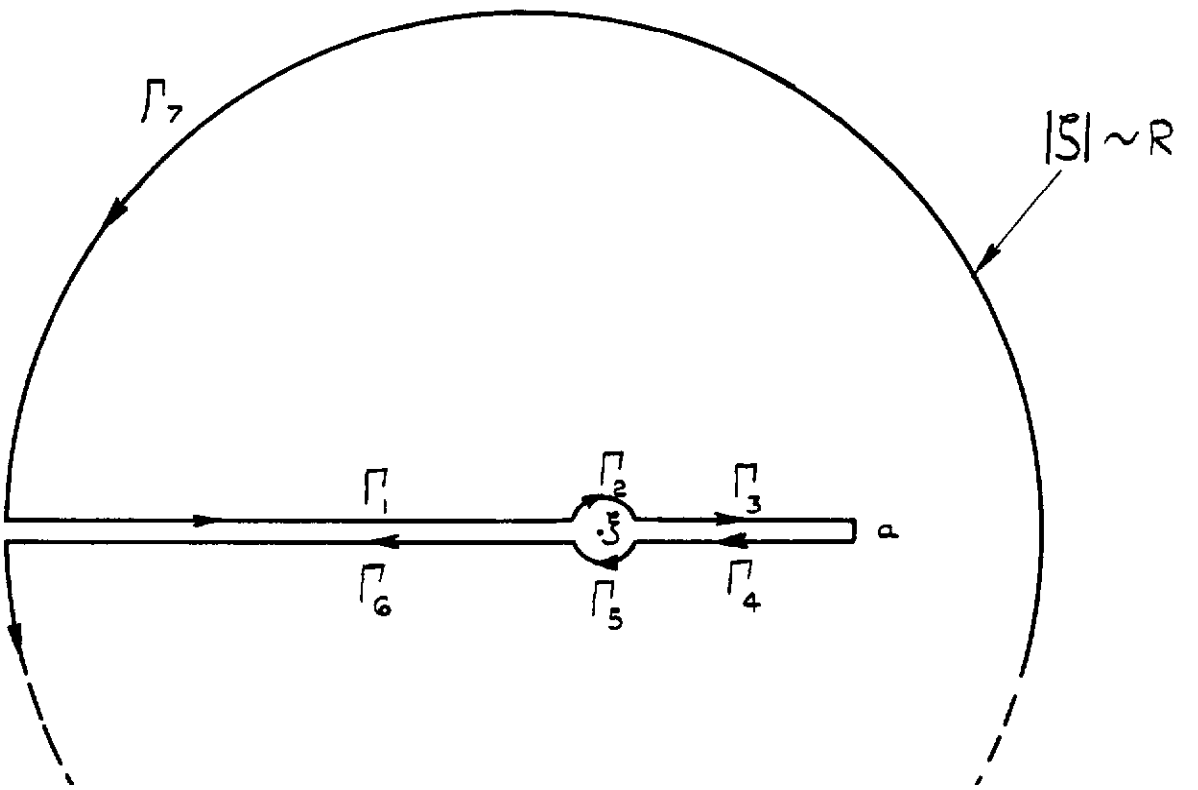

Published by
HER MAJESTY'S STATIONERY OFFICE

To be purchased from
York House, Kingsway, London W.C 2
423 Oxford Street, London W 1
P O Box 569, London S.E.1
13A Castle Street, Edinburgh 2
109 St. Mary Street, Cardiff
39 King Street, Manchester 2
Tower Lane, Bristol 1
2 Edmund Street, Birmingham 3
80 Chichester Street, Belfast
or through any bookseller

PRINTED IN GREAT BRITAIN

S.O. Code No. 23-9009-41